J Mater Sci (2006) 41:8329–8338
DOI 10.1007/s10853-006-1019-2

Effect of microstructure on Young's modulus of extruded Al–SiC composites studied by resonant ultrasound spectroscopy

O. V. Vdovychenko · V. S. Voropaev · A. N. Slipenyuk

Received: 15 July 2004 / Accepted: 21 October 2005 / Published online: 11 November 2006

Abstract In this work, an attempt was made to correlate the Young's modulus of SiC particle reinforced aluminum alloy composites, measured by resonant ultrasound method, to reinforcement spatial distribution. Composites were fabricated by extrusion of billets that were previously formed using cold pressing blend of matrix alloy powders and ceramic particles. It has been shown that more aggregated microstructures were generated with an increase in ceramic volume fraction (to 20%) and the matrix alloy powder mean particle size from 40 to 180 μm as well as with a decrease in the reinforcement particle size (3–14 μm). At the same time, ultrasonic wave velocity as well as Young's modulus diminish with a decrease in SiC content and its particle size, and with increase in matrix alloy particle size. The analysis showed that it could be partly attributed to the higher amount of residual porosity in agglomerated structures. An addition decrease of elastic characteristics was attributed to the increasing influence of mechanically imperfect contacts that formed between ceramic particles in the more aggregated microstructures.

O. V. Vdovychenko (✉) · V. S. Voropaev · A. N. Slipenyuk
Institute for Problems of Materials Science, 3 Krzhyzhanovsky str., Kiev 03680, Ukraine
e-mail: ovdovych@uninet.kiev.ua

Introduction

Metallic composite materials reinforced with ceramic particles or short fibers, known as discontinuously reinforced metal matrix composites (MMCs), have been widely studied over the past few decades. There is a strong potential for these materials to replace existing metallic systems due to their enhanced mechanical properties, especially higher specific stiffness and strength. The possibility of using efficient powder metallurgy (P/M) processes for composite fabrication is also advantageous. A typical P/M route for making discontinuously reinforced MMCs would consist of blending the initial components, pressing the mixture to obtain a compact, consolidation of the compacted material by sintering or hot deformation followed by secondary deformation (e.g. extrusion or rolling) in order to obtain the desired component shape and/or microstructure with acceptable properties. This route allows for the production of isotropic or quasi-isotropic composites with different volume fractions of reinforcement, as well as functionally-graded materials [1, 2] for specific applications.

Improvements in the performance of the current state-of-the-art composite materials may be possible on the basis of detailed studies into the factors affecting their properties. Of particular interest are the following matrix alloy and reinforcement particle characteristics: matrix alloy chemistry and mechanical properties; particle shape [3, 4], mean particle size and size distribution; reinforcement volume fraction [1] and spatial homogeneity of particles distributed in the matrix [5, 6, 7], and density of the consolidated material. The list is not exhaustive. The impact of some of these variables has been well studied and

documented (for example, the effect of the reinforcement volume fraction on elastic modulus [1]), however, others require more extensive investigation. In particular, the effect of the reinforcement distribution on composite properties needs more thorough study, forming the basis for the current work.

In general, the reinforcement distribution in the final material can not be improved by improving the powder mixing process beyond a certain limit. There is a theoretical limit for the homogeneity of the reinforcement spatial distribution, which is primarily controlled by the matrix to reinforcement particle size ratio, or PSR. This limit decreases with increasing PSR i.e. more aggregated structure forms with rise of PSR and the reinforcement volume fraction [8]. At the same time, however, the selection of a certain matrix and reinforcement particle size affects not only the reinforcement spatial distribution (via PSR), but also other material characteristics. For example, particle size affects the amount of stress transfer between matrix and reinforcement, which in turn affects the Young's modulus of the material, as well as machinability etc. Therefore each of these factors should be studied separately, in order to optimize selection of the initial components for composite fabrication.

In this work, the effect of the reinforcement spatial distribution on elastic properties of AlCuMn/SiC_p composites manufactured by P/M is investigated. The aggregation of the ceramic particles in the composites was increased by raising the matrix alloy powder mean particle size (the reinforcement particle size and volume fraction were kept constant) as well as by a decrease in the reinforcement particle size and increase in its volume fraction (i.e. the matrix alloy powder size was kept constant). Such an approach allowed the fabrication of various different composite microstructures, and enabled the effects of microstructure on the material's elastic properties to be studied in detail.

Acoustic measurements [9, 10] in particular resonant ultrasound spectroscopy (RUS) [11–13] has been growing in recent years as a non-destructive technique for determining the elastic moduli of MMCs and to evaluate their microstructural characteristics. Acoustic techniques enable the calculation of all the effective elastic moduli and anelasticity characteristics by measuring the resonant frequencies of the MMC specimen. The RUS method allows these measurements to be carried out using as-extruded samples with simple cylindrical geometries, therefore it was ideally suited for determining the composite Young's modulus in this study. The RUS measurements were performed at the kilohertz frequency range in order to minimize ultrasonic wave scattering by microstructural elements such as particles, pores, and agglomerates. This effect can significantly alter the ultrasonic wave propagation parameters when characteristic size of the microstructural elements and the wavelengths are comparable [14].

Experimental procedure

Fabrication of composites

The composites investigated in this work were made by P/M. Four different gas atomized Al–6Cu–0.4Mn (wt.%) alloy powders were used as the initial matrix materials, with the following powder size fractions: 0–63 μm with a mean particle size of 40 μm; 63–100 μm with a mean particle size of 80; 100–160 μm with a mean particle size of 130 μm and 160–200 μm with a mean particle size of 180 μm. Two different α-SiC powders were used for reinforcement, with average particle sizes 3 and 14 μm respectively.

Powder blends were prepared in a two-stage blending process, using a drum mixer. The process begins with blending in ethyl alcohol for a short time for powder particle de-agglomeration, followed by drying, and then dry mixing for 30 h. Cylindrical billets of diameter 25 mm and length 50 mm were formed from the blended powders using cold pressing at 300 MPa in double-acting steel die. The porosity of the billets at this stage is typically 25–30%. The billets underwent degassing and vacuum forging (hammer strike energy $E_f \approx 7$ kJ, top pressure $P_{max} \approx 1200$ MPa) at 400 °C to obtain consolidate material followed by extrusion at 400 °C. An extrusion ratio of 17:1 (round-to-round) was chosen as the final stage of composite processing, producing fully dense composite rods with a diameter of 6 mm.

Composites were fabricated using the matrix alloy powder size fraction of 0–63 μm (with an average particle size of 40 μm), and reinforced by 5, 10, 15 and 20 vol.% SiC powder with mean particle sizes of 3 and 14 μm. This was done to allow the effects of different reinforcement volume fractions and different reinforcement particle sizes to be observed separately. In addition, composites were also fabricated using matrix alloy powders of average size 40, 80, 130 and 180 μm. These composites were reinforced by 15 vol.% SiC powder with a mean particle size of 14 μm, in order to see the effect of different matrix particle sizes on properties. Un-reinforced matrix alloy samples were also prepared according to the same process, using matrix alloy powders with mean particle sizes of 40 μm and 130 μm.

Microstructural observations were carried out using optical microscopy, on metallographically-prepared specimens obtained from longitudinal sections of the as-extruded materials. The densities of each of the composite samples were measured by the well-established Archimedes technique. Each datum point was obtained by the numerical averaging of three independent measurements. Experimental scatter in these measurements was calculated to be less then 0.5%.

Ultrasonic measurements

Ultrasonic measurements were performed at room temperature using the resonant ultrasound spectroscopy method (RUS) to determine the resonant frequencies of bar specimens under longitudinal oscillations. Two PZT piezoelectric discs having a diameter of 40 mm and height of 2 mm were used as broadband ultrasonic transducers. One transducer excited the specimen, and the opposite transducer transformed the mechanical response into an electrical signal that was first amplified before being analyzed. A distinctive feature of the present method in comparison with conventional RUS-technique [10, 15] is the absence of mechanical interaction between the ultrasonic transducers and the specimen. The specimen was suspended between the transducers by a thin rubber sheet that was fixed in the middle of the long dimension of the specimen. A drop of mineral oil was applied in the gap between each transducer and the specimen to provide the acoustic contact. This minimizes the influence of edge conditions on the natural frequencies of the bar, since the bar specimen middle section is a node of the fundamental oscillation (and all subsequent odd modes) and therefore has no displacement. At the same time, the specimen face displacements are free.

Cylindrical samples of between 50 and 60 mm in length and 6 mm in diameter were used for the measurements. The resonant frequencies of the first three modes of longitudinal oscillation were determined using an oscilloscope. The resultant ultrasonic velocity was averaged over three measurements, with the error in the measurements not exceeding 0.5%.

The velocity of ultrasonic wave propagation is given by [16]

$$C_{\mathrm{b}} = 2l \cdot f_n \cdot n^{-1}, \tag{1}$$

where l is the sample length, and f_n is the frequency of the nth mode of resonance.

Young's modulus E was then calculated as [17]

$$E = C_{\mathrm{b}}^2 \rho, \tag{2}$$

where ρ is the experimentally determined density. It should be noted that the Poisson's ratio is absent in this equation, in contrast to the elastic formulation for longitudinal ultrasonic waves propagating in an isotropic medium (see Eq. 4). This problem is also generally seen in the case of porous materials, whose Poisson's ratio—porosity dependence is ambiguous at best [18, 19], which makes accurate Young's modulus determination by widespread pulse methods very difficult in these materials. A more accurate formula, which also takes into consideration the transverse motion of the bar elements during longitudinal oscillation, is given by [16]

$$E = C_{\mathrm{b}}^2 \rho \left(1 - \frac{n^2 v^2 \pi^2 r^2}{4l^2}\right)^{-2} \tag{3}$$

where l and r are the specimen length and radius, respectively, n is the number of resonant oscillation mode, and v is the Poisson's ratio. However, analysis of Eqs. 2 and 3 shows that for an isotropic aluminum bar with length-to-radius ratio of 10 and Poisson's ratio of 0.34, the difference between Young's modulus values calculated according expressions (2) and (3) does not exceed 0.06%. It is possible that a decrease of Poisson's ratio due to porosity and/or increases in ceramic volume fraction further reduces this difference. In light of this, Eq. 2 was used for the Young's modulus calculation.

Results

Microstructural observations

Figures 1–3 show optical micrographs of polished cross sections from the composites studied in this work. The dark angular particles represent SiC particles in the micrographs. In Fig. 1, micrographs are presented for composites containing SiC particles having an average size of 3 μm. For materials containing 5 and 10 vol.% SiC particles (Fig. 1a and b respectively) the reinforcement distribution is quite uniform. Although it is possible to reveal a few clusters of particles that are not separated by matrix layers, significant particle agglomeration is not observed. However, an increase in the reinforcement volume fraction to 15 vol.% (Fig. 1c) leads to large SiC particle agglomerations. These particle agglomerations tend to flake off when preparing the metallographic sections because the formation

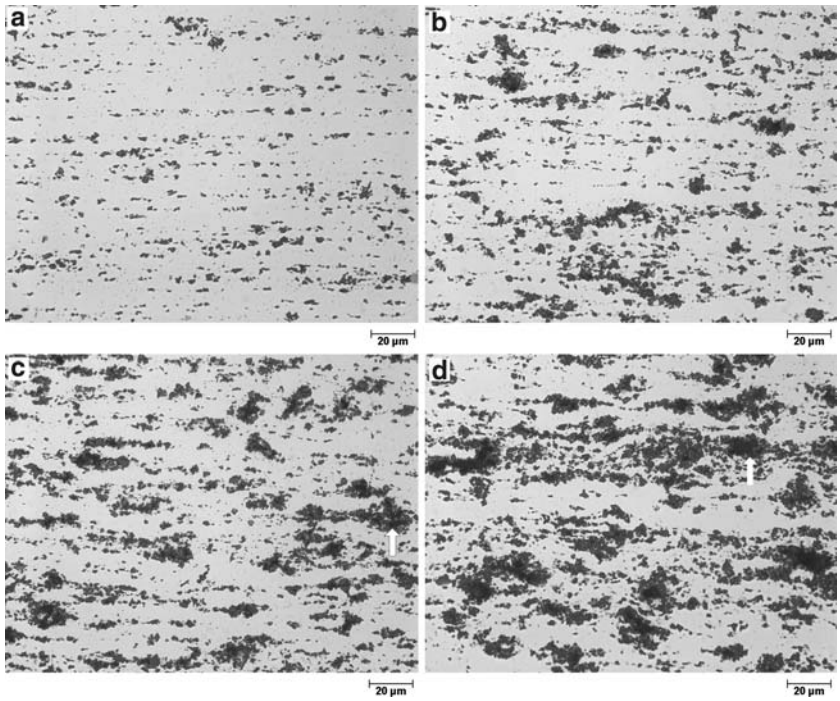

Fig. 1 Reinforcement distribution in Al–Cu–Mn (40 μ*m* mean particle size)/ SiC (3 μ*m* mean particle size) composites: (a) 5 vol.% SiC, (b) 10 vol.% SiC, (c) 15 vol.% SiC, (d) 20 vol.% SiC

of a strong bond between SiC particles is impossible under the present processing conditions without the presence of a matrix alloy interlayer. The white arrows on Fig. 1 mark the voids that have formed after particles have flaked off during polishing. Particle agglomeration becomes even more obvious with an increase in SiC volume fraction to 20 vol.% (Fig. 1d).

The tendency to form reinforcement particle clusters significantly decreases as the SiC particle size is increased to 14 μm in comparison with the 3 μm SiC particles, and large agglomerates are not observed even in the composites reinforced with 20 vol.% SiC particles having an average size of 14 μm (Fig. 2).

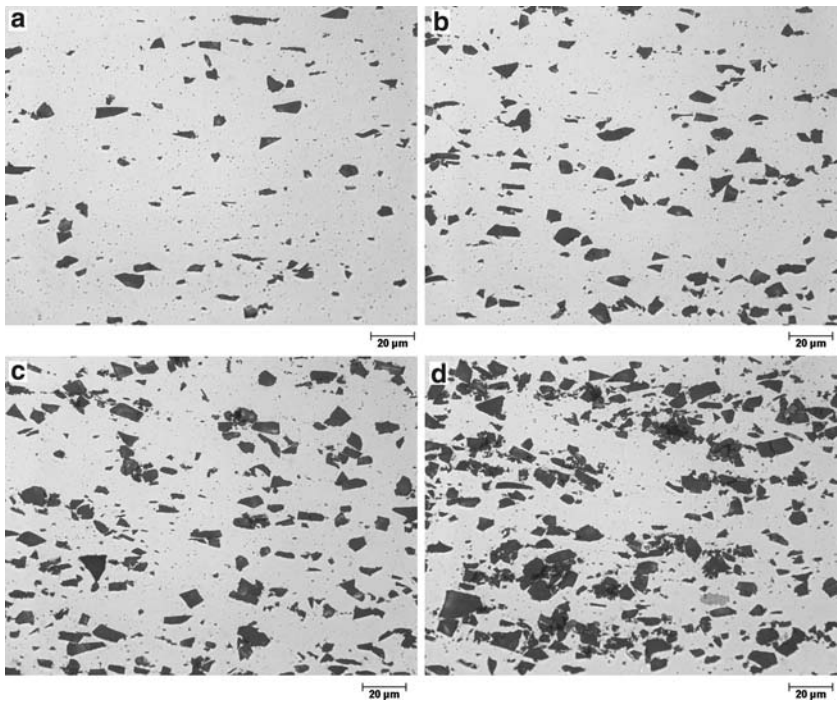

Fig. 2 Reinforcement distribution in Al–Cu–Mn (40 μ*m* mean particle size)/ SiC (14 μ*m* mean particle size) composites: (a) 5 vol.% SiC, (b) 10 vol.% SiC, (c) 15 vol.% SiC, (d) 20 vol.% SiC

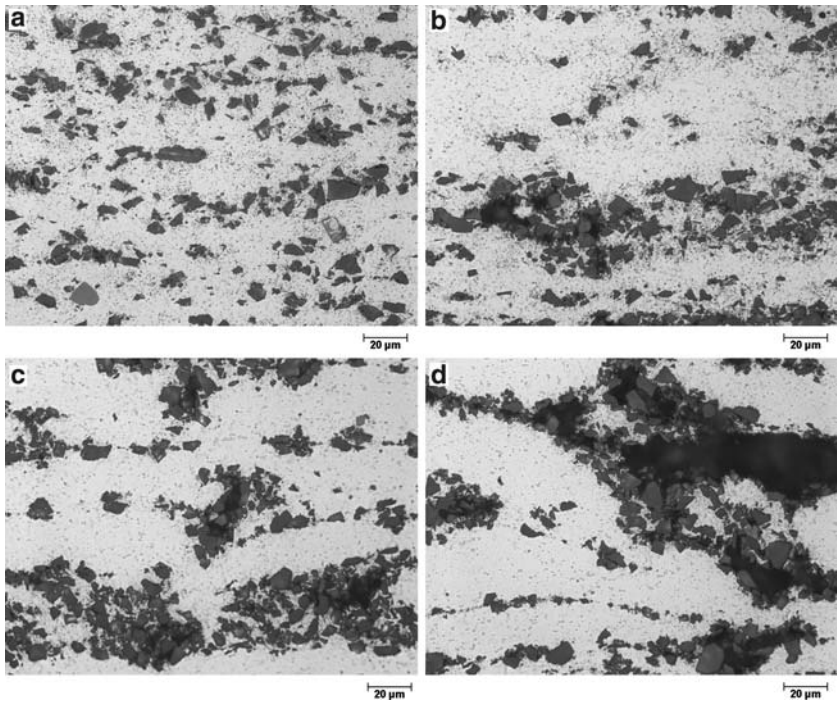

Fig. 3 Reinforcement distribution in Al–Cu–Mn/SiC (15 vol.%, 14 μ*m* mean particle size) composites. Mean particle size of the matrix alloy powder: (a) 40 μ*m*, (b) 80 μ*m*, (c) 130 μ*m*, (d) 180 μ*m*

The specimens containing equal amounts of identical reinforcement particles (15 vol.%, 14 μm SiC) prepared from different size fractions of the matrix powder (i.e. initial average particle sizes ranging from 40 to 180 μm) were studied to show the influence of SiC agglomeration on composite elastic properties, independent of volume fraction and particle size effects. The microstructures of composites prepared in this way are shown in Fig. 3. The material based on matrix alloy powder with particle initial average size of 40 μm does not generally contain SiC clusters (Fig. 3a), but an increase in initial average size of matrix powder even to 80 μm results in a marked deterioration in the homogeneity of SiC particle spatial distribution, leading to the formation of SiC particle clusters (Fig. 3b). Furthermore, Fig. 3c and d clearly indicate that materials prepared from coarser matrix powders tend to develop a significantly more aggregated microstructure than samples obtained from finer matrix powders.

Ultrasonic velocity measurements

The experimental velocity measurements for longitudinal waves in the composite bar specimens are plotted in Figs. 4 and 5. From Fig. 4, it can be observed that for both reinforcement particle sizes, higher ultrasonic wave velocity is found in the samples with the highest SiC volume fraction. Furthermore, longitudinal wave velocity increases faster with increasing SiC content in materials containing coarse reinforcement particles compared with finer SiC particles. This difference is virtually absent for composites containing 5 vol.% of reinforcement however, it becomes more evident with increase in the amount of SiC. For example, at 15 vol.% SiC content, the specimens prepared using 14 μm ceramic powder have a 4% higher longitudinal wave velocity than those prepared using 3 μm reinforcement powder. A similar effect is also seen for composites containing 20% SiC.

Additionally, the initial size of the matrix alloy powder also affects the longitudinal wave velocity measured in the composite specimens. Interestingly,

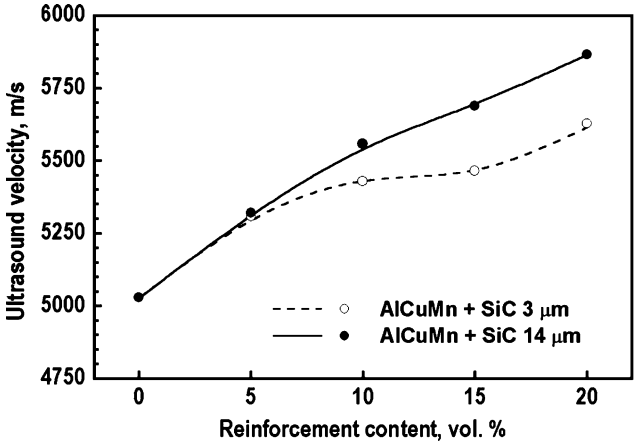

Fig. 4 Effect of reinforcement content on velocity of longitudinal ultrasonic waves in the composites

this effect is not seen in the materials without reinforcement. As can be seen in Fig. 5, the longitudinal wave velocity in composites containing 15% SiC (14 μm) decreases as the average matrix powder size increases from 40 to 180 μm. The wave velocities measured in materials prepared from 40 μm aluminum alloy powder are about 7% higher than those measured in materials prepared from 180 μm powder. This increase in longitudinal wave velocity is of comparable magnitude with the increase due to 15% SiC reinforcement addition.

Density measurements

Figures 6 and 7 show the results of density measurements for matrix materials and composites. Figure 6 clearly shows that the composite density does not change monotonically with increasing SiC volume fraction, as expected. For composites containing 5% SiC, the density increase is approximately in accordance with the rule of mixtures (ROM). However, at SiC volume fractions greater than this, there is a maximum and then a decrease in density. A more detailed analysis reveals a strong influence of SiC particle size on the density of the composite. At 5% SiC content, the densities of the composites containing different sized SiC particles are very similar. As can be seen from the figure, the densities of those composites containing 14 μm SiC particles are closer to the ROM estimate than those containing 3 μm SiC, which tend to be significantly lower. For example, the density values for composites containing 15% and 20% volume fraction of 3 μm SiC are both lower than the base aluminum alloy density.

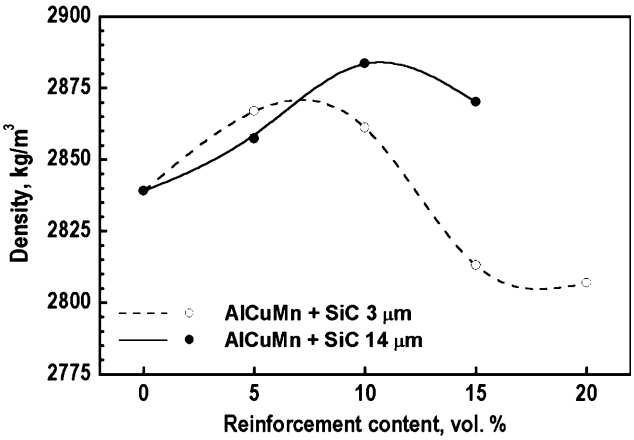

Fig. 6 Effect of reinforcement content on density of P/M processed Al–Cu–Mn/SiC particle reinforced composites

Figure 7 also shows that for the composite containing 15 vol.% of 14 μm SiC particles, the density decreases with increasing matrix powder size, while the density of the un-reinforced matrix remains virtually unchanged. The 15% SiC composite prepared from 180 μm matrix powder 14 μm SiC powder has a lower density than the matrix material. These experimental data clearly indicate residual porosity in some of the composite materials.

Discussion

In this work, the velocity of elastic wave propagation was measured experimentally by using the RUS technique for composite bar specimens of finite dimensions. However, much of the literature uses an unbounded medium approximation to estimate the

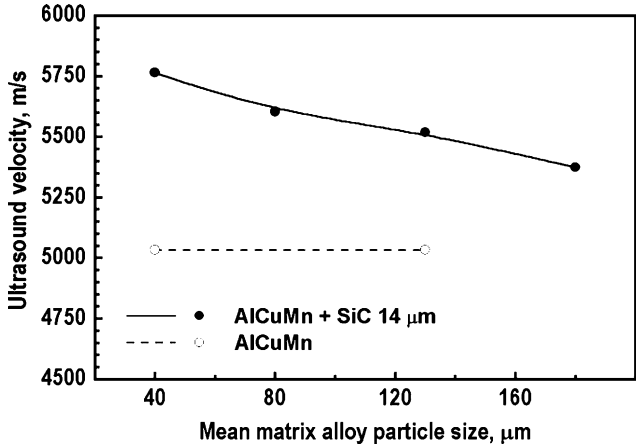

Fig. 5 Effect of mean matrix alloy particle size on velocity of longitudinal ultrasonic waves in the composites

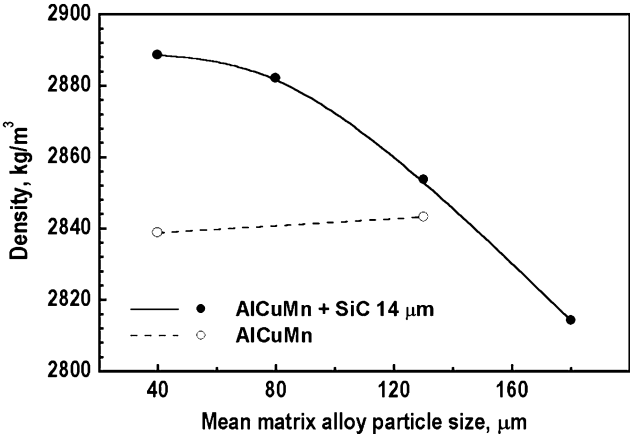

Fig. 7 Effect of mean matrix alloy particle size on density of P/M processed Al–Cu–Mn/SiC particle reinforced composites

velocity of longitudinal ultrasonic wave propagation. Therefore, a direct comparison between our experimental data (Figs. 4 and 5) and previous results for ultrasonic wave propagation in aluminum/SiC composites (for example, Gür and Ogel [10]) may not be appropriate. Therefore, in order to compare our results with those from previous works [10], an additional expression [17] relating the longitudinal wave velocity in an unbounded medium (C_l) with the characteristics of the elastic medium must be used:

$$C_l = [E(1-\nu)/\rho(1+\nu)(1-2\nu)]^{1/2} \quad (4)$$

Here, E is the Young's modulus, ν is the Poisson's ratio and ρ is the density. Comparing this expression with Eq. 2 gives for isotropic materials:

$$C_b = C_l\left(\frac{(1+\nu)(1-2\nu)}{1-\nu}\right)^{1/2} \quad (5)$$

where C_b is the ultrasonic wave velocity measured in the bar specimens. From Eq. (5), for a material with $\nu = 0.35$ (i.e. Poisson's ratio of aluminum) we find that $C_l/C_b \approx 1.27$. The unbounded medium ultrasonic wave velocity (C_l) has previously been measured in a hot-pressed (600 °C) aluminum alloy prepared from pure Al powder (180 μm) and 5wt.% Cu [10, 20]. The ratio between this velocity C_l and C_b measured in the present work for the P/M matrix material is about 1.28, indicating that the P/M route produces a matrix material with a similar Young's modulus to that of the alloy prepared at the higher temperature, which almost certainly formed a liquid phase during processing. Unfortunately, there is no data for Poisson's ratio or porosity of the Al–SiC composites produced in the previously cited paper [10]. A more detailed comparison between elastic wave propagation velocities in these two studies is therefore not possible.

As can be seen from the data presented in Figs. 6 and 7, the composites containing more than 10 vol.% SiC are porous. The density of a composite of porosity θ is given by

$$\rho_c = \rho_m(1 - V_i^\theta - \theta) + \rho_i V_i^\theta \quad (6)$$

where ρ_m, ρ_i and ρ_c are the density of the matrix material, the inclusions and the composite as a whole, respectively, and V_i^θ is the inclusion volume fraction in the porous composite. Assuming that the total volume of inclusions and matrix materials remains unchanged (i.e. the inclusion volume fraction in the solid phase stays the same), V_i^θ can be written:

$$V_i^\theta = V_i(1-\theta) \quad (7)$$

where V_i is the inclusion volume fraction in solid phase. From Eqs. 6 and 7 one obtains the following equation for porosity:

$$\theta = 1 - \frac{\rho_c}{\rho_m(1-V_i) + \rho_i V_i} \quad (8)$$

where ρ_c is the experimentally determined density of the composite, ρ_m and ρ_i are the density of the matrix and inclusions, respectively, and V_i is the volume fraction of inclusions.

Figure 8 shows Young's modulus values calculated from our experimental data using the formula (2). The data show that the effective Young's modulus of the composites increases with the volume fraction of the inclusions. Figure 8 also includes a mean-field prediction for Young's modulus of Al–SiC composites, as proposed by Wakashima et al. [9, 21]. This model allows for elastic interaction between inclusions, i.e. the condition of a dilute concentration of the second phase is relaxed. The Young's modulus mean-field prediction was calculated using Eq. 9 [17]:

$$E_{mfm} = \frac{9K_{mfm}G_{mfm}}{3K_{mfm} + G_{mfm}} \quad (9)$$

For spherical second-phase particles, the mean-field model gives

$$K_{mfm} = K_m + (K_i - K_m)\frac{V_i K_m a}{(1-V_i)K_i + V_i K_m a}, \quad (10)$$

and

$$G_{mfm} = G_m + (G_i - G_m)\frac{V_i G_m b}{(1-V_i)G_i + V_i G_m b}, \quad (11)$$

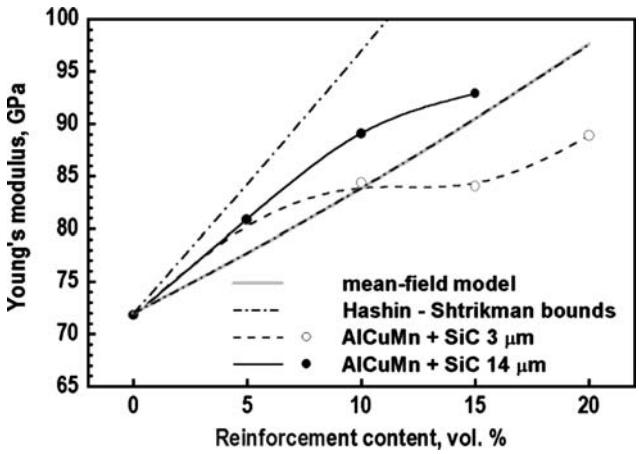

Fig. 8 Effect of reinforcement content on Young's modulus of P/M processed Al–Cu–Mn/SiC

where K and G are the bulk and shear moduli, respectively, and

$$a = \frac{K_i(3K_m + 4G_m)}{K_m(3K_i + 4G_m)} \tag{12}$$

$$b = \frac{G_i[6G_m(K_m + 2G_m) + G_m(9K_m + 8G_m)]}{G_m[6G_i(K_m + 2G_m) + G_m(9K_m + 8G_m)]}. \tag{13}$$

The values of E_{mfm} plotted in Fig. 8 were calculated as a function of inclusion volume fraction, using a bulk modulus for α-SiC of K_i = 220 GPa, and a shear modulus of G_i = 200 GPa [22]. The matrix bulk and shear moduli, K_m and G_m, were calculated from the experimentally determined value of matrix Young's modulus E_m = 72 GPa, assuming a matrix Poisson's ratio of ν_m = 0.34. Figure 8 also demonstrates that the mean-field model prediction for the case of spherical inclusions agrees with the Hashin–Shtrikman lower bound [23] for a macroscopically isotropic two-phase composite with inclusions of arbitrary shape. As can be seen in Fig. 8, the Young's modulus experimental data lie quite close to this theoretical prediction. However, the Young's modulus of the composites reinforced with > 5% coarser particles is higher than that for composites with finer inclusions, as was also seen in the ultrasonic wave velocity data. Figure 9 indicates that the Young's modulus for composites containing 15% of 14 μm SiC decreases as the matrix powder size increases. Taking into account the density data, conclusions can be drawn into residual porosity effects on the composite elastic modulus and ultrasonic wave velocity in these materials.

However, it has previously been reported [24–26] that the ultrasonic velocity and Young's modulus of P/M materials may be affected not just by pore fraction, θ, but also by pore morphology, particle–particle contact and the presence of cracks. In order to verify the influence of porosity on composite elastic properties, the zero-porosity Young's moduli of composites reinforced by SiC 15 vol.% (14 μm) were calculated using the generalized self-consistent scheme, first derived by Mackenzie [27] for spherical non-interacting pores:

$$E_{gscs} = E^{\theta}\left[1 + \theta\frac{3(1 - \nu_{mfm})(9 + 5\nu_{mfm})}{2(7 - 5\nu_{mfm})}\right] \tag{14}$$

where E_{gscs} denotes the Young's modulus of a composite with zero porosity, E^{θ} is the experimental determined value of the composite Young's modulus, θ is the porosity, calculated using Eq. 8 and ν_{mfm} is the Poisson's ratio of the zero porosity composite, determined using the following relationship [17]:

$$\nu_{mfm} = \frac{3K_{mfm} - 2G_{mfm}}{2(3K_{mfm} + G_{mfm})} \tag{15}$$

where the bulk and shear moduli K_{mfm} and G_{mfm} are calculated using Eqs. 10 and 11, respectively. Values of E_{gscs} are plotted in Fig. 9. It is noteworthy that values of E_{gscs} virtually coincide with the Young's modulus of composites with zero porosity calculated using Hashin–Shtrikman upper bound formula for porous materials [23]:

$$E_{HS} = E^{\theta}\left(\frac{1}{1 - \theta}\right)\left(1 + \frac{(1 + \nu_{mfm}) \cdot (13 - 15\nu_{mfm}) \cdot \theta}{2 \cdot (7 - 5\nu_{mfm})}\right). \tag{16}$$

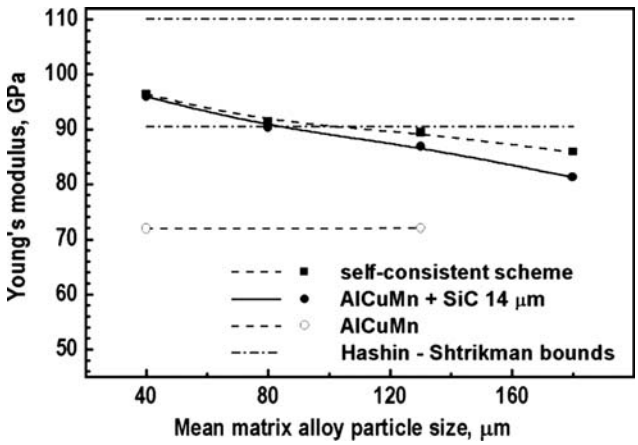

Fig. 9 Effect of mean matrix alloy particle size on Young's modulus of P/M processed Al–Cu–Mn/SiC particle reinforced composites

The data suggest that the decrease in Young's modulus (and, consequently, in the ultrasonic velocity) is caused not only by the residual porosity, but also by other additional factors, some of which have been suggested previously.

According to the data shown in Figs. 5 and 7, both the density and the ultrasonic velocity in the matrix are independent of the aluminum alloy matrix powder size. It is reasonable, therefore, that the elastic properties of the matrix remained unchanged with changing particle size. There is no information about SiC particle size effect on its Young's modulus. However, the Young's modulus values of the composites that contain 5 vol.% of 3 μm and 14 μm particles (Fig. 8) virtually coincide. Again, for materials with equal reinforcement particle sizes, the change in Young's modulus cannot be caused by difference in the inclusion properties (Fig. 9).

Previous work [28] has established that the processing steps used to fabricate the materials used in this study should provide near-perfect bonding between the matrix alloy particles. Moreover, the mechanical treatment results in embedding of angular ceramic particles into the matrix and formation of near-perfect (mechanically) contacts between the matrix and the SiC particles. One possible explanation of the decrease in Young's modulus as the matrix—reinforcement particle size ratio (PSR) increases is therefore the presence of imperfect contacts between ceramic particles, caused by its agglomeration. During the initial processing steps, the SiC particles are mainly situated on the surfaces of the matrix powder particles. Increasing the matrix particle size leads to a decrease in the specific surface area of the matrix powder, which increases the spatial heterogeneity of the SiC particle distribution and, consequently, promotes particle agglomeration. Increasing the reinforcement volume fraction also results in the promotion of ceramic particle agglomerates, which can contain pores. Correspondingly, both the residual porosity and the number of ceramic–ceramic inter-particle contacts increase. The behavior of these particle aggregates under loading is similar to the behavior of granular media. However, experimental and theoretical works [24, 29, 30] show that elastic wave velocities and, respectively, the elastic moduli of granular materials (including green and partially sintered powder materials) are substantially less than that of basic condensed materials with the same porosity. This deviation is attributed to peculiarities of the inter-particle contact deformation therefore increasing the matrix alloy particle size leads to a further reduction in the composite Young's modulus. The tendency for inclusion particle agglomeration is higher for composites with higher PSR. As the reinforcement content is increased, therefore, there is a greater reduction in Young's modulus for the composites containing 3 μm SiC than those containing 14 μm SiC. To illustrate this point, we compare the composite containing 3 μm SiC particles at volume fractions of 10% and 15%. The decrease in Young's modulus due to these combined effects is roughly the same as the increase in Young's modulus expected from the increase in volume fraction from 10% to 15%, hence the Young's modulus values are similar in both composites.

Conclusions

Ultrasonic wave velocities and Young's moduli of P/M composite materials extruded from aluminum alloy and silicon carbide powders were determined as functions of reinforcement volume fraction and also matrix and inclusion powder particle size, using the RUS technique. Although changes in composite Young's modulus over a range of reinforcement volume fractions of 0–20% can be approximated by Wakashima mean-field model, there are significant deviations from this theory prediction. Microstructural analyses indicate that these composites tend to develop more spatially-heterogeneous (aggregated) microstructures for higher matrix—reinforcement particle size ratios (PSRs) and higher volume fractions of reinforcement. The spatial homogeneity of the SiC particle distribution is found to affect density, ultrasonic wave velocity and Young's modulus in these composites. The elastic constants of composites from the same aluminum alloy powder with average particle size (40 μm) and containing > 5 vol.% SiC are higher in materials with coarser inclusions (14 μm vs. 3 μm). Conversely, the ultrasonic velocity and Young's modulus decrease with increasing matrix particle size in composites containing 15 vol.% SiC (14 μm) although the elastic constants of the pure matrix remain practically unchanged over the same range of particle size. Since highly agglomerated microstructures are more likely to contain high residual porosity, this decrease in Young's modulus can be attributed to influence of porosity. As suggested by the zero-porosity modulus calculation using the generalized self- consistent scheme, the decrease in Young's modulus with matrix particle size is greater than would be expected based on specimen porosity alone. An additional decrease was attributed to the increasing influence of mechanically imperfect contacts that formed between ceramic particles in the more spatially heterogeneous (aggregated) microstructures.

Acknowledgements This work was partially supported by Science and Technology Center in Ukraine (P061 project). The authors also express their sincere gratitude to Dr. Jonathan E. Spowart of UES, Inc., for helpful suggestions and assistance in preparing the manuscript.

References

1. Clyne TW, Withers PJ (1993) An introduction to metal matrix composites. University Press, Cambridge
2. Suresh S, Mortensen A (1998) Fundamentals of functionally graded materials processing and thermomechanical behaviour of graded metals and metal-ceramic composites. University Press, Cambridge
3. Spowart JE, Miracle DB (2003) Mater Sci Eng A357:111
4. Song SG, Shi N, Gray III GT, Roberts JA (1996) Metall Mater Trans 27A:3739

5. Slipenyuk A, Kuprin V, Milman Yu, Spowart JE, Miracle DB (2004) . Mater Sci Eng A381:165
6. Spowart JE, Ma Z-Y, Mishra RS (2003) In: Jata KV, Mahoney M, Mishra RS (eds) Friction stir welding and processing, TMS, Warrendale Press
7. BhanuPrasad VV, Bhat BVR, Mahajan YR, Ramakrishnan P (2002) Mater Sci Eng A337:179
8. Kusy RP (1977) J Appl Phys 48:5301
9. Kang C-S, Maeda K, Wang K-J, Wakashima K (1998) Acta Mater 46:1209
10. Gür CH, Ogel B (2001) Mater Character 47:227
11. Vdovychenko O (2003) in Proceedings of the international conference ''Novel technology in powder metallurgy and ceramics'', Kiev, September 2003, IPMS, Kiev, p 389
12. Migliori A, Sarrao JL (1997) Resonant ultrasound spectroscopy. Wiley, New York
13. Vdovychenko OV (1994) Ph.D. Thesis, National Academy of Science of Ukraine
14. Papadakis EP (1965) J Acoust Soc Am 37:703
15. Lee T, Lakes RS, Lal A (2000) Rev Sci Instrum 71:2855
16. Kuzmenko VA (1963) Sonic and ultrasonic oscillations used for materials dynamic tests. Academy of Science of USSR, Kiev, (in Russian)
17. Landau LD, Lifshitz EM (1986) Course of theoretical physics. Theory of elasticity, vol 7, 3rd edn. Pergamon Press, Oxford
18. Roberts AP, Garboczi EJ (2002) Proc R Soc Lond A458:1033
19. Ramakrishnan N, Arunachalam VS (1993) J Am Ceram Soc 76:2745
20. Ogel B, Gurbuz R (2001) Mater Sci Eng A301:213
21. Wakashima K, Tsukamoto H (1991) ibid A146:291
22. Schreiber E, Anderson OL, Soga N (1973) Elastic constants and their measurements. McGraw-Hill, New York
23. Hashin Z, Shtrikman S (1963) J Mech Phys Solids 11:127
24. Goddard JD (1990) Proc R Soc Lond A430:105
25. Kachanov M (1999) Int J Fracture 97:1
26. Mukhopadhyay AK, Phani KK (2000) J Eur Ceram Soc 20:29
27. Mackenzie JK (1950) Proc Phys Soc (London) 63B:2
28. Voropaev VS, Vdovychenko OV, Slipenyuk AN (2004) Metallofiz Noveishie Tekhnol 26:831
29. Vdovychenko OV, Podrezov YuN (2005) Metallofiz Noveishie Tekhnol 27:1429
30. Schilling CH, Garcia VJ, Smith RM, Roberts RA (1998) J Am Ceram Soc 81:2629